ACS OMEGA

Open Access

http://pubs.acs.org/journal/acsodf

Article

Cold Plasma for the Modification of the Surface Roughness of Microparticles

Hale Oguzlu,* Alberto Baldelli, Xanyar Mohammadi, Albert Kong, Mattia Bacca, and Anubhav Pratap-Singh

Cite This: *ACS Omega* 2024, 9, 35634−35644

Read Online

ACCESS | Metrics & More | Article Recommendations

ABSTRACT: Cold plasma treatment is commonly used for sterilization. However, another potential of cold plasma treatment is surface modification. To date, several efforts have been directed toward investigating the effect of cold plasma treatment in modifying the surfaces of films. Here, the impact of suspension properties and parameters of cold plasma treatment on the changes of surfaces of monodisperse polymeric microparticles is tested. The plasma treatment did not touch the surface chemistry of the monodisperse polymeric microparticles. The concentration of suspensions of 1 mg/mL was determined to relate to a stronger effect of the plasma treatment on the roughness of the microparticles. Microparticles with an average diameter of 20 μm show a roughness increase with the plasma treatment time. However, a plasma treatment time longer than 15 min damages the microparticles, as observed in particles with an average diameter of 20 and 50 μm. We finally prototyped monodisperse microparticles to deliver drugs to the nasal mucosa by studying the effect of roughness in their (undesired) self-adhesion and (desired) adhesion with tissue. A moderate roughness, with an average peak-to-valley distance of 500 nm, appears to be the most effective in reducing the detachment forces with nasal tissue by up to 5 mN.

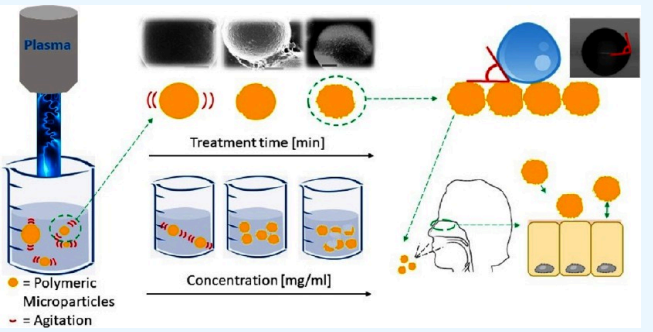

1. INTRODUCTION

Cold plasma treatment is a technique commonly used in food and pharmaceutical science for sterilization for deactivating germs, bacteria, pathogens, or fungi.[1] Plasma ions destroy the walls of bacteria or spores or the proteins of viruses acting, thus, of interest as a sterilization tool.[2] Cold plasma removes organic compounds and portions on the surface in materials like plastic or polymers, usually creating hydrophobic surfaces. The removal of part of the surface material seems to be derived from the agitation or the beam energy.[3] Low-temperature plasma procedures take advantage of the narrow focus of the beam and the strong effect on different bacteria strains, making it more efficient.[4] It has been demonstrated that cold plasma procedures can damage microbial DNA and surface structures.[5] Moreover, several studies applied cold plasma techniques to kill airborne viruses, which raises interest due to the recent pandemic. For instance, Filipić et al. demonstrated that cold plasma techniques can deactivate almost all types of enteric viruses, such as norovirus, adenovirus, and hepatitis A virus, while dispersed in water.[6] As with many techniques, the efficiency of cold plasma in sterilization comes with limitations. Some examples are a reduction in color, a surge in the oxidation of lipids, an increase in acidity, a diminishment in the firmness of fruits, and a degradation of thermolabile medical devices.[3,6−8] The strongest challenge in using cold plasma techniques is poor control. In fact, the control of the reaction mechanism is subjected to the reactive species contained in the plasma state.[9−11] It is worth noting that scaling up is also challenging, making the cold plasma technique poorly applicable for bulk production.[12]

Even with its challenges, the technique of cold plasma has been intensively investigated for bacteria or virus deactivation. However, there is a minority of references that sought cold plasma as an alternative application.[10,13] There are two main applications of cold plasma, namely, the synthesis of nanoparticles and surface modification. Nanoparticles, made of metal, such as gold or silver, or made of starch, have been successfully created using a vacuum cold plasma, and several references extensively discussed the optimization of the cold plasma parameters in achieving the desired nanoparticle size.[14−19] Similarly, several references introduced the use of

Received: April 19, 2024
Revised: July 12, 2024
Accepted: July 18, 2024
Published: August 1, 2024

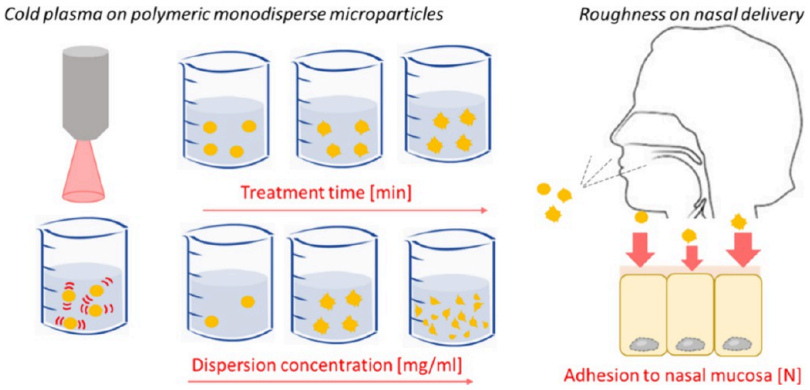

Figure 1. Representation of the two main goals of this study. (1) Analysis of the effect of cold plasma timing and dispersion concentration on the surface morphology of polymeric monodispersed microparticles. It is expected that both variables can have an effect in increasing the surface roughness of polymeric microparticles dispersed in water. (2) The behavior of monodisperse polymeric microparticles with different roughness on the process of adhesion to the nasal mucosa. Based on previous references, an average microroughness is expected to generate the lowest adhesion forces.

cold plasma to modify the surface of several materials, such as fibers of packaging films.[3,8,20,21] Cold plasma showed an effect in altering several characteristics of the surface of a material. Surface charge and roughness appeared to be impacted when the materials were exposed to a cold plasma beam.[9] For example, the surface roughness of organic materials highly increases after exposure to a cold plasma treatment.[22] Also, the cold plasma impacts the roughness of films; through physical and chemical etching, this treatment increases the roughness and the contact angle with aqueous solutions.[7] The ability of cold plasma to control the surface properties of films is highly desirable for packaging among other applications. For instance, several innovative films have been created recently using Zein, a class of prolamine protein found in corn (maize).[12,23,24]

To the authors' knowledge, cold plasma's effect on microparticles' surface roughness is currently unexplored, making this project novel. The ability of cold plasma treatments to control the surface chemistry and roughness in monodisperse microparticles has a significant impact on several research areas. For instance, monosized polymeric microbeads are extensively used in biological and medical applications as carriers, such as in cell separation and immunoassays, in nuclear medicine for diagnostic imaging, in site-specific drug-delivery systems, in affinity separation of biological entities, and in studying the phagocytic process.[25] Microspheres are also employed as bulking agents or as embolic or drug-delivery particles.[26] Monodisperse polymeric microparticles are produced by electrospray, atomization, emulsion cross-linking, precipitation, microfluidics, and 3D printing.[27] However, the techniques cannot be used to add controlled roughness on the surface of monodisperse polymeric microparticles. Monodisperse spray drying or atomization could be used; however, not on polymers but on salts or sugars.[28] Furthermore, scaling up cold plasma treatment for generating monodisperse polymeric microparticles can be overcome due to the low microparticles needed for certain studies.

For example, monodisperse polymeric microparticles with identical surface properties can be used to study the adhesion between inhalable drugs and the nasal mucosa.[29] In particle engineering, polymers with high molecular weight encapsulate otherwise fragile drugs. Therefore, the shell formed by a polymer would predominantly lead to the adhesion between inhalable microparticles and nasal mucosa.[30] Currently, the experimental work related to the adhesion between microparticles and a flat surface is limited due to the complexity of the required techniques.[28,31,32] Even more limited is the evaluation of the impact of inhalable microparticles' morphological properties on the nasal mucosa's adhesion. While it is well known that the material properties, such as mucoadhesivity, of inhalable microparticles' surfaces are fundamental for efficient nasal delivery, other morphological aspects have been poorly investigated.[33−35] For example, the size of inhalable microparticles is linked to the deposition location, suggesting important physical scaling. As previously observed, inhalable microparticles with a diameter between 50 and 150 μm deposit mostly in the nasal cavity.[28,36] Furthermore, surface roughness can affect microparticles' self-adhesion and microparticles' adhesion to the nasal tissue.[37] While the influence of the size on the delivery of inhalable nasal microparticles has been highly determined,[38] the impact of roughness has been poorly investigated experimentally. A deeper investigation of the impact of roughness on the efficacy of nasal delivery could highlight the importance of engineering and tuning inhalable microparticles. The abovementioned physical scaling involves adhesion, which is known to be impacted by surface roughness.[39,40] Hence, there is a need for control of the surface finishing of these particles. The procedures commonly used to produce monodisperse microparticles are suspension, emulsion, dispersion, and sedimentation polymerization.[26] These methods usually involve surfactants or detergents as stabilizers, which can create hazardous chemical waste. In addition, these methods tend to produce mostly monoshaped or smooth microspheres. Further introducing surface roughness in these microparticles can generate chemical waste or require complicated chemical procedures.[41,42] Using cold plasma to create monodisperse rough polymer microparticles is beneficial and innovative thanks to reducing or eliminating the side effects observed in the competing techniques. We also analyzed a critical application of polymeric monosized microparticles: the adhesion of these particles to the nasal mucosa for nasal drug delivery. A visual representation of the cold spray technique and its use in microparticles for nasal delivery is reported in Figure 1.

https://doi.org/10.1021/acsomega.4c03787
ACS Omega 2024, 9, 35634−35644

2. MATERIALS AND METHODS

2.1. Microparticles. Nonfunctionalized polystyrene (CAS No. 500-008-9) microparticles were purchased from Alpha-Nanotech with 50, 20, and 5 μm diameters. These microparticles showed a nonfunctionalized surface. Microparticles were dispersed in water (>99%, CAS No. 231-791-2). Three concentrations of the microparticles were later prepared: 0.5, 1, and 5 mg/mL. The reason for having different concentrations is to verify the impact of the cold plasma technique on the surface of dispersed monosized microparticles made of polystyrene. Therefore, a matrix of nine formulations, including three different concentrations and sizes of the microparticles, were tested. Dispersions of microbeads were placed in glass vials with a height of 5 cm and a diameter of 20 mm. The vials were filled with microparticle dispersion.

2.2. Surface Treatment. An open-air cold plasma treatment system (PlasmaTreat) was used to modify microparticles' surface roughness. The parameters used for all of the formulations were a distance between the vial and plasma probe of 1 cm and a temperature of 25 °C. The distance was selected to avoid drops from the dispersion to the plasma probe. More considerable distances were not considered since a lower effect of the plasma treatment on the microparticles was expected.[11,24] The effect of the plasma time is the only parameter that was tested. Different times were considered: 0, 1, 5, 15, and 20 min.

2.3. Characterization Techniques. *2.3.1. Effect of the Plasma Treatment on Dispersions of Monosized Microparticles. 2.3.1.1. Morphology.* Dried microparticles were placed on a scanning electron microscopy (SEM) stub, on which double-sided tape and a filter (0.2 μm pore size and 13 mm diameter, GSWP04700, EMD Millipore, Etobicoke, ON, Canada) were attached. The samples were covered with a 3 nm layer of gold using a coat sputter (Cressington 208HR High-Resolution Sputter Coater, Cressington Scientific Instruments Ltd., Watford, UK). A Helios NanoLab 650 Focused Ion Beam Scanning Electron Microscope (SEM; FEI Company, Hillsboro, Oregon, USA) was used under 13 mA and 5 kV conditions. Previous publications described this imaging procedure in more detail.[43−45] The gold sputtering procedure was normalized so that the SEM could be used for a qualitative analysis of the roughness, as explained in a previous reference.[46]

The project area equivalent diameter (d_a) was extracted by analyzing the SEM images. We then used ImageJ software to analyze the visual data. More details on the SEM analysis for extraction of d_a are listed in previous publications.[43]

The profile and surface roughness of treated and nontreated microparticles were analyzed using two confocal microscopes, an Olympus LEXT OLS3100 and an Olympus FV1000 Laser Scanning/Two-Photon Confocal Microscope. The first was to generate a 3D profile useful for qualitative comparison. The second one was used to derive the average roughness (R_a).

2.3.1.2. Stability. The electrostatic or charge repulsion and attraction between particles was measured through the zeta potential. The last has been analyzed by using a Litesizer 500 Particle Size Analyzer. Before analyzing zeta potential, suspensions were exposed to a 5 min agitation using a sonication bath. This process was performed for only this test. More experimental details are shown in a previous reference.[47] The surface chemistry of nontreated and treated microparticles' stability was verified using Fourier transform infrared spectroscopy (FTIR). Suspensions were dried in a vacuum chamber for 2 days at room temperature. The FTIR was used in the attenuated total reflection mode. Therefore, the dispersion of microparticles was dried in a vacuum oven overnight. We used approximately 0.1 g of a dry powder. The typical spectrum of polystyrene beads is reported in a previous publication.[48] The main peaks in polystyrene beads are the following: between 3000 and 3030 cm^{-1}, aromatic C−H stretching vibration absorption can be detected, while between 1400 and 1650 cm^{-1}, we found aromatic C═C stretching vibration absorption. Between 500 and 1050 cm^{-1}, we observe C−H out-of-plane bending vibration absorption, while between 2000 and 3000 cm^{-1}, the presence of methylenes is previously reported.[48,49]

2.3.2. Behavior of Rough Monosized Microparticles in the Nasal Environment. The contact between monosized polystyrene microparticles and the nasal environment has been tested by analyzing the contact angles between nanoparticles and simulated nasal mucus and the adhesion forces between microparticles and nasal tissue.

The contact angle was measured using a custom-made static contact angle measurement technique. Microparticles have been homogeneously distributed on a silicon wafer by depositing a droplet of 50 μL of dispersion of 5 mg/mL of monodisperse polymeric microparticles. The homogeneity of the layer was verified by using a SEM. The static contact angle was considered as the average of different time steps, each second for 5 s, of the contact angle of a droplet of 25 μL placed on a flat surface covered with microparticles. The contact angle was measured using ImageJ, as described in previous publications.[50]

The adhesion to the nasal tissue is fundamental for nasal delivery. The experimental procedure for determining the adhesion forces has been explained in a previous work.[51] Briefly, the adhesion between monosized polystyrene microparticles and the nasal tissue of a healthy donor (ethic approval number H22-02336 and obtained through an endoscopic endonasal surgery) from the tissue culture reserve at the Providence Airway Centre (PAC) funding sponsored by Providence Health Care, was examined using a Texture analyzer, TA-XT2 (Stable Micro Systems Ltd., Surrey, U.K.), with experimental conditions of velocity pretest 50 mm/s, test 50 mm/s, post-test 10 mm/s, tracking 5 mm/s, test force 20 g, trigger force 10 g, return distance 4 mm, and contact time 5 s. Previous publications showed the experimental method in detail.[51−54] A double-sided adhesive disk was used to adhere 100 mg of powder to a cylindrical tube (Hoseney dough stickiness rig). The excess powder was removed with gentle shaking. The monodispersity of the powder was checked with a microscope. The nasal tissue was placed in a plastic container using double-sided tape; the container was placed on the stage of the texture analyzer. The container was filled with simulated nasal mucus (BZ253, Bio Chemazone, 3000−5000 cP). The thickness of the simulated nasal mucus was measured to be 3 mm, the average in a healthy individual.[55]

2.4. Statistical Approach. The statistical approach differed according to the property characterized. For instance, when deriving the d_a, we studied 300 particles. The standard errors were obtained by producing the standard deviations of the 300 measurements. For all of the other properties, the experiments were repeated three times. We performed a statistical analysis of the results using a t test or ANOVA.

https://doi.org/10.1021/acsomega.4c03787
ACS Omega 2024, 9, 35634−35644

Table 1. Images at Two Different Scales of the Monosized Polystyrene Microparticles Treated with Cold Plasma at Other Times: 0, 1, 5, 15, and 20 min[a]

5 μm			
[min]\ [mg/ml]	0.5	1	5
0	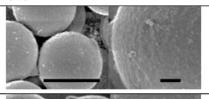	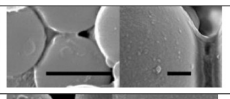	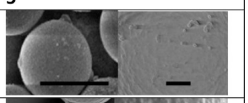
1	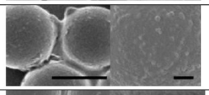	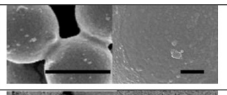	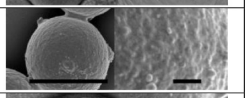
5	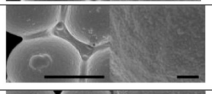	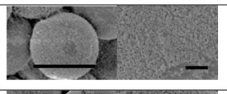	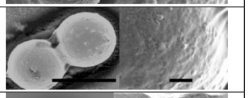
15	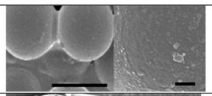	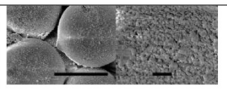	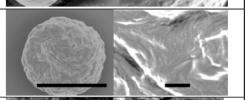
20	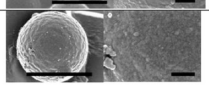	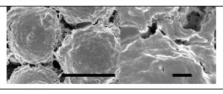	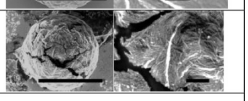
20 μm			
[min]\ [mg/ml]	0.5	1	5
0	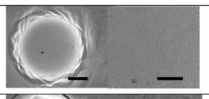	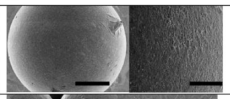	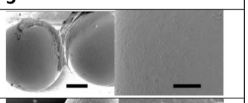
1	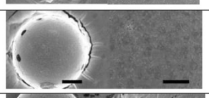	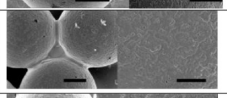	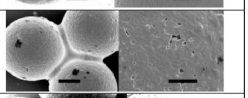
5	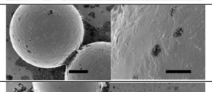	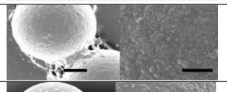	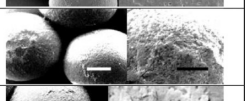
15	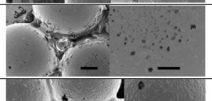	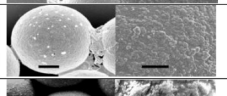	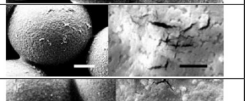
20	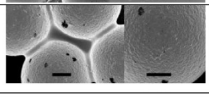	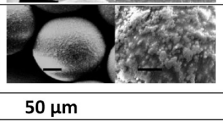	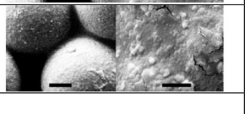
50 μm			
[min]\ [mg/ml]	0.5	1	5
0	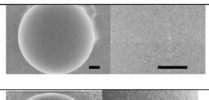	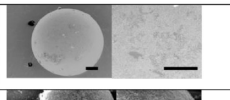	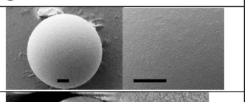
1	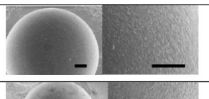	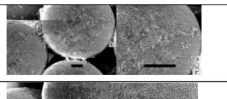	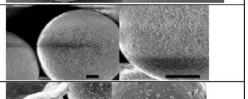
5	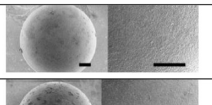	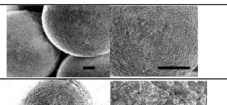	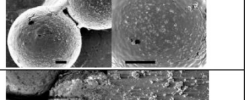
15	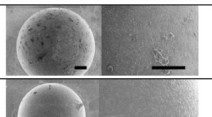		
20			

[a]Microparticles were dispersed in a dispersion at different concentrations, 0.5, 1, and 5 mg/mL. The scale bars indicate 5 μm and 500 nm, respectively.

3. RESULTS AND DISCUSSION

3.1. Effect of the Plasma Treatment on Dispersions of Monosized Microparticles. The morphology is the first parameter commonly verified in the establishment of the effect of any treatment. In this study, plasma-treated microparticles are images using a SEM. In Table 1, we show two pictures, taken at different magnifications, for every case of polymeric monodisperse microparticles treated and nontreated with a cold plasma at different processing times. The change in the surface structure of microparticles of different average diameters according to the plasma processing time is visible. In most cases, the surface of nontreated microparticles appears smooth and clean. Most of the imperfections in this case are related to the sputtered material layer. By increasing the processing time, the surface assumed a rougher appearance. In particular, irregular structures can be more visible at high processing times, such as 15 or 20 min. As happens with films and surfaces, the plasma beam etches the surface of

https://doi.org/10.1021/acsomega.4c03787
ACS Omega 2024, 9, 35634−35644

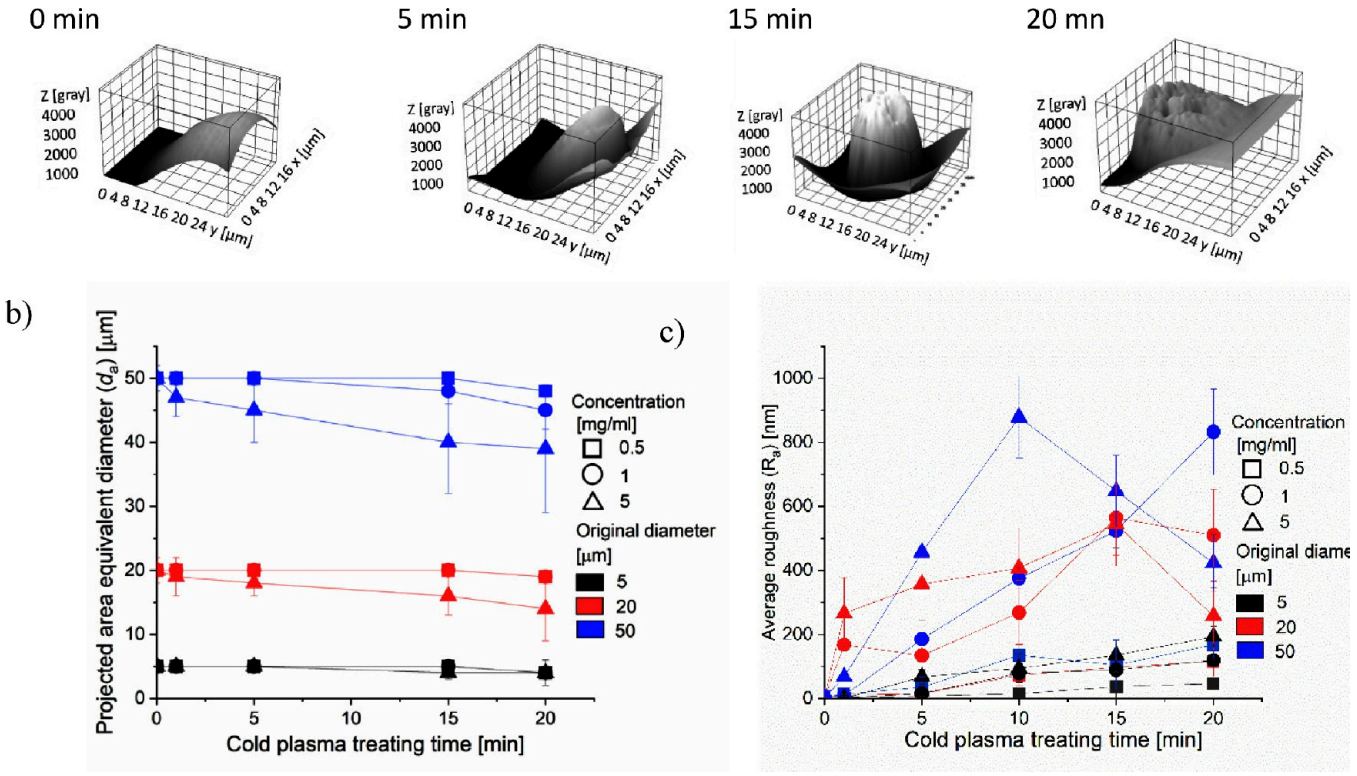

Figure 2. In (a), some examples of the 3D profiles are shown. They relate to polymeric monodisperse microparticles of 50 μm and 1 mg/mL treated with plasma at different times. In (b), the size distribution of the microparticles treated with plasma treatment with respect to different diameters of microparticles and different concentrations of the microparticles' dispersion. In (c), the average roughness of the microparticles treated with plasma treatment with respect to different diameters of microparticles and different concentrations of the microparticles' dispersion.

monodisperse polymer microparticles.[7] Better visual support for the increase in roughness concerning the increase in processing time can be seen in Figure 2 a, where we report the 3D profiles. At the 20th min of processing time, microparticles with a diameter of 50 μm and a concentration of 1 mg/mL are much rougher than the nontreated ones.

The etching procedure might affect the particle size. While removing material is removed from the surface, the average diameter of the microparticles can decrease. A slight decrease can be seen for every case considered, as shown in Figure 2 b). The etching effect of the cold plasma treatment can also be detected in films. In polyurethane films and with an etching time of 10 s, Sanchis et al.[56] determined a reduction of a few nanometers in thickness. The etching effect of plasma treatment was also verified with weight loss; after 20 min, each polyurethane film lost an average of 150 $\mu g/cm^3$.[56] The average roughness of polyimide film treated with oxygen-cold plasma for 5 min increases by 13-fold.[57] The same effect can also be observed in monodispersed polymeric beads, as shown in Figure 2c). However, the relationship between average roughness and treatment time is not linear for all of the cases analyzed. For microparticles with an average diameter of 5 μm, with an increase in etching time, there is an increase in the average roughness, even if minor. For microparticles with diameters of 20 and 50 μm, treatment times of 20 min are related to a drastic decrease in roughness with respect to the cases with a treatment time of 10 min. The decrease is, on average, 30% higher when the microparticle concentration is 5 mg/mL, compared to the case of 1 mg/mL. This can indicate that for higher treating times and higher concentrations, the microparticles tend to bounce and hit each other, potentially leading to rupture. This hypothesis can be verified by observing the images for the case of 50 μm, 5 mg/mL, and 20 min (Figure 1). In this case, some free materials can be noticed between microparticles. The damage derived by the bouncing effect can be noticed on suspensions treated by other processes, such as an ultrasonic probe. In this case, the probe generates a vibration that makes the microparticles hit each other and, for polymeric microparticles, the damage of some microparticles.[58,59] The effect of cold plasma treatment on monodisperse microparticles might not be permanent, as indicated in a previous study.[60]

Different types of plasma treatment can impact not only the surface morphology but also the surface chemistry. Therefore, the chemical composition of polymeric monodisperse microparticles was tested via zeta potential and infrared spectroscopy. The zeta potential is identified as a physical property that manages electrostatic interactions in particle dispersions and is fundamental in understanding the stability of suspensions.[61] Based on the results from zeta potential, cold plasma treatment is peeling off the layers from microparticles without possibly, creating any surface group.[62−64]

The analysis of the vibrational modes has been conducted using an FTIR. A few samples have been shown in Figure 3 due to the similarity of several curves. The analysis of the vibrational modes of plasma-treated microparticles identified one trend. At higher plasma treating times, there is a broad peak in the C−H stretching area centered at the wavelength of 3400 cm^{-1}. A similar effect can be recognized in a previous study, where polystyrene microparticles are treated with phosphoric acid.[65] In this previous study, the cause of this broad peak is claimed to be due to sulfonated polystyrene.[65]

https://doi.org/10.1021/acsomega.4c03787
ACS Omega 2024, 9, 35634−35644

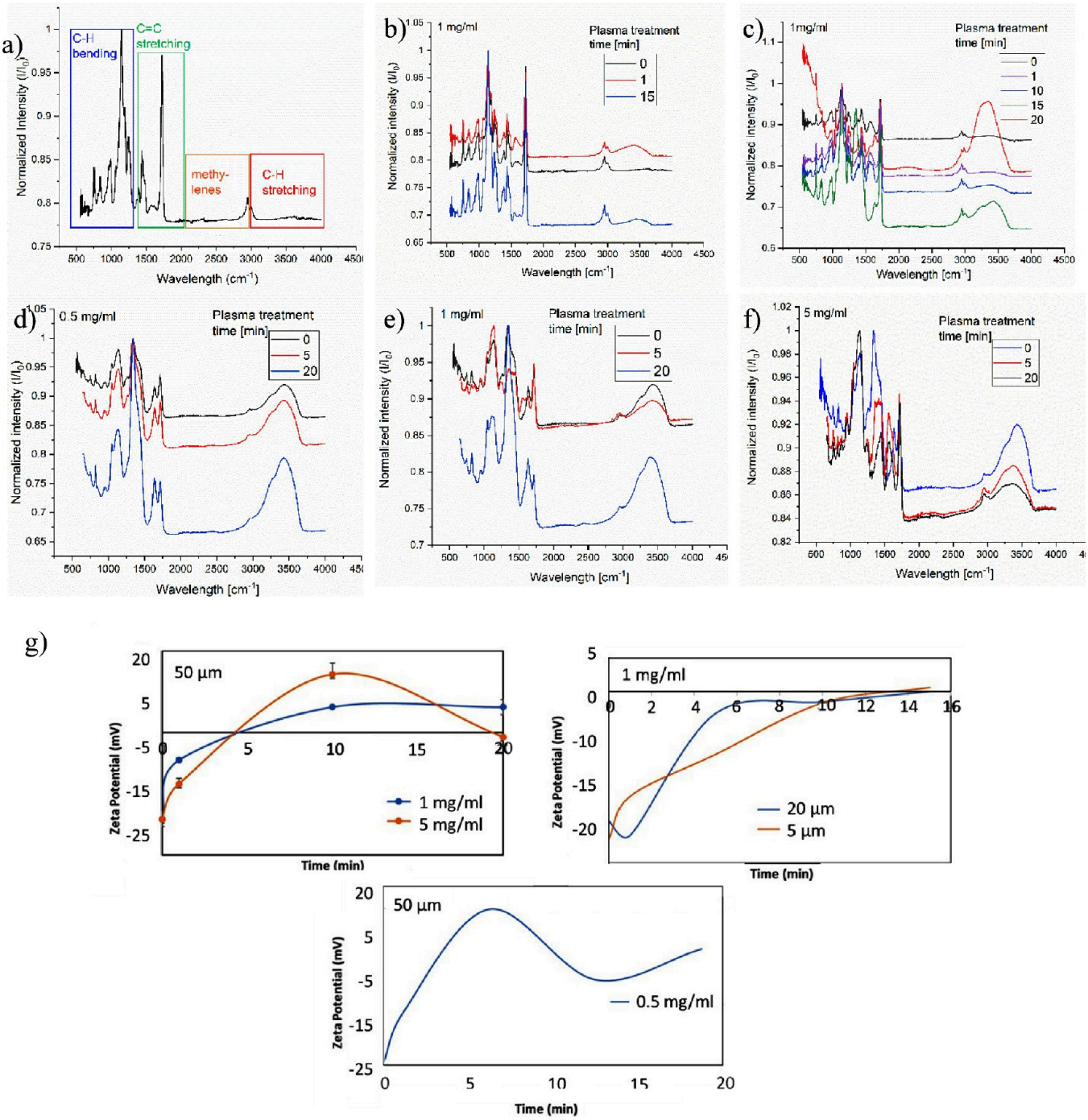

Figure 3. Infrared spectra of (a) untreated microparticles of a diameter of 5 μm with an explanation of the meaning of each group of peaks, (b) of the plasma-treated microparticles of 5 μm and 1 mg/mL, (c) of the plasma-treated microparticles of 20 μm and 1 mg/mL, (d) of the plasma-treated microparticles of 50 μm and 0.5 mg/mL, (e) of the plasma-treated microparticles of 50 μm and 1 mg/mL, and (f) of the plasma-treated microparticles of 50 μm and 5 mg/mL. (g) Zeta potential values of untreated and treated microparticles of a diameter of 5 μmm, 20 μmm, and 50 μm.

Since this cannot be the case in this study due to the lack of any sulfur-based compound, the same peak can also be found in polystyrene foams.[66,67] This peak is also typical of larger polystyrene microparticles, underlining a possible correlation between the microparticles' size and the peak area at 3400 cm^{-1}.[48]

As a consequence, there might be an influence of cold plasma treatment on the surface chemistry of the polystyrene microparticles. However, the lack of changes in infrared (IR) spectra of the same particle size, 50 μm, and different concentrations, as shown in Figure 3, underlines that such change appears minor. In addition, minor changes are visible in the zeta potential trend in time, as shown in Figure 3g.

3.2. Behavior of Rough Monosized Microparticles in the Nasal Environment. The second aim of this article is to understand the relationship between the surface properties of polymeric monodisperse microparticles and the simulated nasal mucus layer. The hydrophobicity of microparticles and

https://doi.org/10.1021/acsomega.4c03787
ACS Omega 2024, 9, 35634−35644

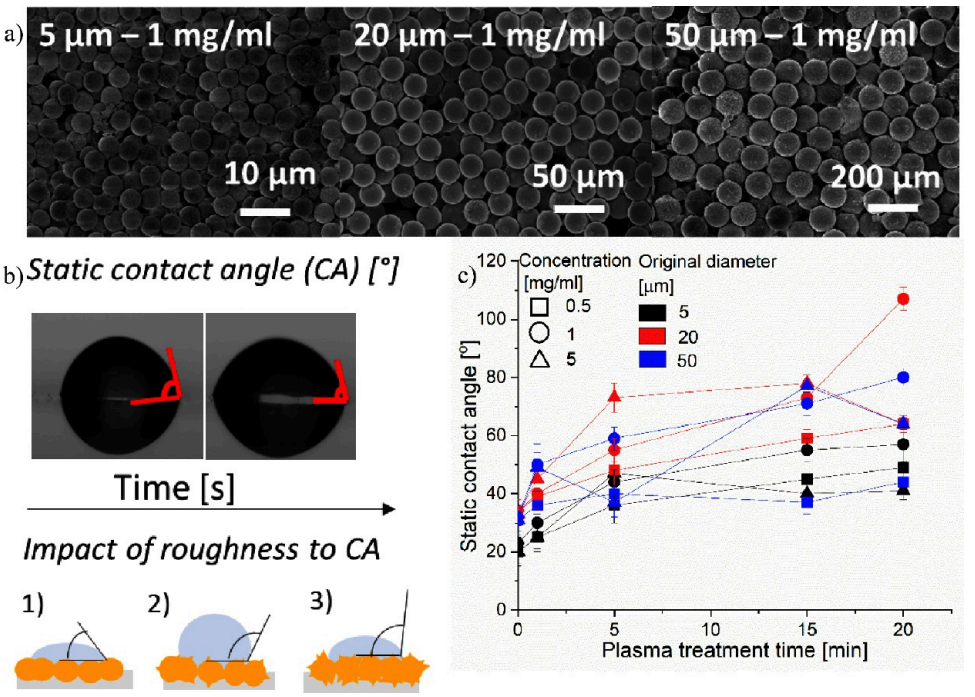

Figure 4. Behavior of the contact between microparticles and artificial simulated nasal mucus. (a) Images of surfaces fully covered with monodisperse microparticles used in the contact angle measurements. (b) Examples of the static contact angle and the impact of roughness on the hydrophobicity are shown. (c) The trend of the static contact angle with respect to the concentration of monodisperse microparticles and the diameter of monodisperse microparticles is illustrated.

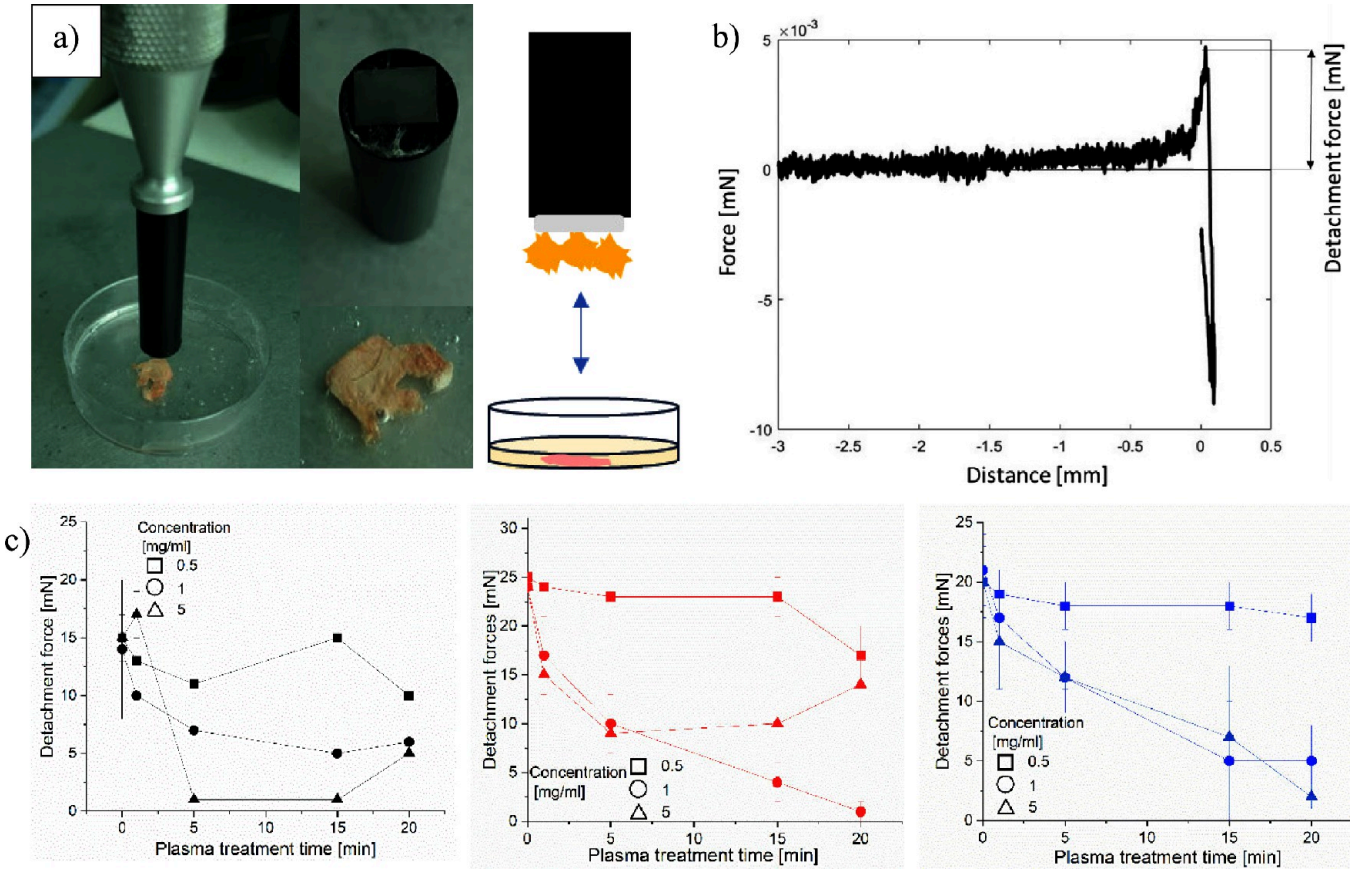

Figure 5. (a) Pictures of the experiments using the texture analyzer are shown along with a sketch of the experiment. (b) An example of the curve of the detachment forces of monodisperse plasma-treated microparticles. (c) The trend of the detachment forces with respect to the concentration and size of plasma-treated monodisperse microparticles.

https://doi.org/10.1021/acsomega.4c03787
ACS Omega 2024, 9, 35634−35644

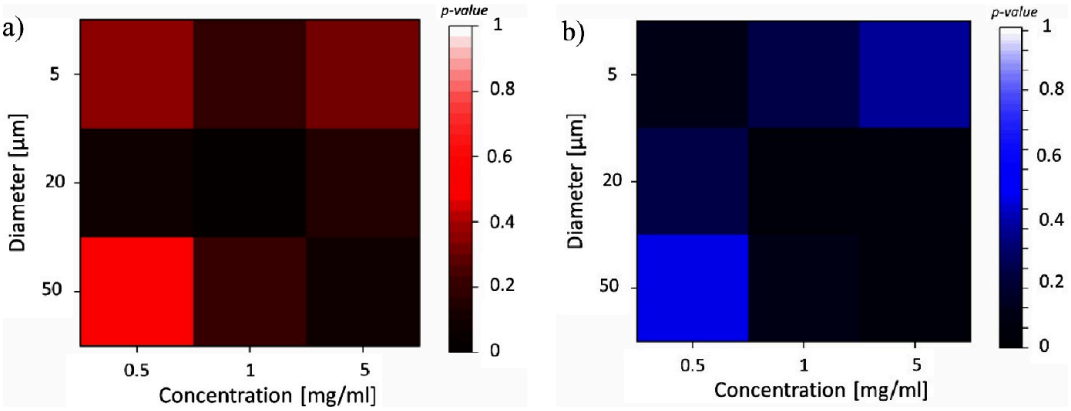

Figure 6. Correlation between roughness and contact angle trends in (a) and between the trends of roughness and adhesion in (b) achieved using a one-way ANOVA. The concentration identifies the quantity of particles dispersed in water.

the mucoadhesion forces of microparticles on nasal tissue have been analyzed to characterize this relationship. Hydrophobicity is commonly measured through the contact angle of an even surface and a water droplet. The simulated nasal mucus is composed of about 95% water. Therefore, the simulated nasal mucus can be assumed to behave similarly to water. The smoothness of the surface is important, since any imperfection could affect the results.[50] Therefore, microparticles were distributed on the surface homogeneously, as shown in Figure 4a. Assuming a homogeneous surface, air cavities and roughness are the main factors influencing material hydrophobicity.

Consequently, in a layer of microparticles, the diameter of the microparticles and the roughness are the main properties linked to hydrophobicity. In the case of 5 μm as the diameter of microparticles, the spacing between two consecutive microparticles can be considered to be smaller than in larger microparticles. However, in microparticles with an average diameter of 50 μm, the spacing can be large enough to allow water droplet penetration. Therefore, we expect higher hydrophobicity in microparticles with 20 μm in average diameter (Figure 4 b). This is confirmed by the trend in contact angle versus plasma treatment time, as shown in Figure 4c. The other factor influencing hydrophobicity is surface roughness, where a higher roughness is expected to generate large contact angles against water droplets. This positive trend is confirmed by Figure 4c; however, the slope reduces as the roughness increases, and in some cases, we see an opposite trend.[68] In this case, the distance between each peak of the etched surface of microparticles can be large enough to allow water penetration, leading, thus, to lower values of contact angle (Figure 4).[69,70]

Another important variable to determine the influence of surface roughness on monodisperse polymer microparticles for nasal delivery is their detachment force. As in the case of contact angle measurement, a homogeneous layer of microparticles was prepared for these tests, and examples of the layer are shown in Figure 4a. These microparticle layers were deposited on silicon wafers, which were attached to a probe (1 cm in diameter) of a texture analyzer, as shown in Figure 5a. As shown in Figure 5a, we reproduced the microenvironment of the nasal cavity. The nasal cavity consists of nasal tissue and a few μm layers of nasal mucus. The microparticles were slowly placed in contact with the nasal mucus layer and retracted once they touched the tissue. The force necessary to detach the microparticles from the nasal tissue was measured and labeled as detachment force, as shown in Figure 5b. The force has been estimated to be the difference between the time zero and the highest detachment value encountered (Figure 5b). For long plasma treatment times, the detachment forces are almost always lower, and we speculate that this is due to the connection between roughness and adhesion. A higher surface roughness commonly allows a weaker bond with soft surfaces.[71,72] A lower surface area of contact can give a lower adhesion, thus penalizing rough microparticles, due to the limit in contact between roughness peaks.[28] The connection between roughness and adhesion is emphasized by the cases of 20 μm in particle diameter and 20 min of treatment time. In these cases, higher treatment times reduce the roughness due to particle bouncing. This reduction in roughness produces a reduction in detachment forces, as shown in Figure 5c. Particle concentration in the dispersion does appear to impact the detachment forces of microparticles with nasal tissues significantly. Lower particle concentrations produce fairly smooth microparticle surfaces at different plasma treatment times; thus, the detachment forces are about 15% lower than 1 and 5 mg/mL cases. However, the case of 1 mg/mL appeared to show a stronger etching effect at different plasma treating times. As previously explained, this effect is even stronger for microparticles with an average diameter of 20 μm.

3.3. Influence of the Surface Properties on Nasal Tissue Adhesion. Plasma treatment has been indicated as a powerful tool to control the surface roughness of microparticles without strongly affecting the surface chemistry. While the plasma treatment time seems, in most cases, to have a linear relationship with the surface roughness of the particles and with the adhesion forces with nasal mucus, the concentration of the microparticle suspension and the diameter of the microparticle show a more complicated trend. Based on the correlation between roughness, diameter, and concentration, the case shows the highest roughness for a concentration of 1 mg/mL and a diameter of 20 μm. The 1 mg/mL concentration appears optimal, giving the highest benefit in microparticle treatment. Lower concentrations can reduce the effect of plasma treatment on some of the dispersed microparticles. Larger concentrations can lead to the bouncing of microparticles and reduce the global effect of plasma treatment on the microparticles with some resulting damage. Particles with a diameter of 20 μm are mostly affected by the treatment. Particles of smaller diameters have a reduced surface

https://doi.org/10.1021/acsomega.4c03787
ACS Omega 2024, 9, 35634−35644

area between themselves and the liquid, thus reducing the effect of the plasma treatment. Particles with larger diameters instead might tend to localize the effect of plasma treatment on the surface of the suspension, as observed from the high standard deviations in the roughness measurements. The roughness of monodisperse microparticles appears to impact their detachment forces from artificial mucus. The samples showing lower detachment force also have the highest roughness, as shown in Figure 6b.

4. CONCLUSIONS

We prototyped cold plasma treatment to control the surface properties of monodisperse polymeric microparticles. Our investigation shows that processing time has the highest impact on the results. Long (between 10 and 15 min) plasma treatment times produce enhanced surface roughness within a certain range, where excessive processing time (above 15 min) has been shown to produce some damage to the microparticles (due to mutual collisions). The concentration and diameter of the microparticles also have an important effect on their surface properties. While cold plasma treatment shows a poor influence on the surface chemistry, we observed a significant impact on the surface roughness. The optimal treatment conditions for the microparticles are observed for a concentration of 1 mg/mL and an average diameter of 20 μm, where we see a linear trend between plasma treatment time and surface roughness. We then correlate treatment time and surface roughness with the detachment force between the particles and nasal tissues, with simulated nasal mucus, and the contact angle of the particles. Our study included a limited range of concentrations and average microparticle diameter. Future investigations can expand our study to include a wider range of these properties, a deeper analysis of the surface chemistry, and prototype cold plasma treatments in rough monodisperse microparticles for broader applications.

AUTHOR INFORMATION

Corresponding Author

Hale Oguzlu − *Faculty of Dentistry, Department of Oral Biological and Medical Sciences, University of British Columbia, Vancouver V6T 1Z4, Canada; Sustainable Functional Biomaterials Laboratory, Department of Wood Science, The University of British Columbia, Vancouver, British Columbia V6T 1Z4, Canada; School of Chemical Engineering, The University of Queensland, Brisbane, Queensland 4072, Australia;* orcid.org/0000-0003-0984-7040; Email: oguzlu@ualberta.ca

Authors

Alberto Baldelli − *School of Agriculture and Food Sustainability, The University of Queensland, Brisbane 4072, Australia; Queensland Alliance for Agriculture and Food Innovation, The University of Queensland, Brisbane 4067, Australia; Faculty of Food and Land Systems, The University of British Columbia, Vancouver V6T 1Z4, Canada;* orcid.org/0000-0002-6296-5460

Xanyar Mohammadi − *Faculty of Food and Land Systems, The University of British Columbia, Vancouver V6T 1Z4, Canada*

Albert Kong − *Department of Mechanical Engineering, The University of British Columbia, Vancouver V6T 1Z4, Canada*

Mattia Bacca − *Department of Mechanical Engineering, The University of British Columbia, Vancouver V6T 1Z4, Canada*

Anubhav Pratap-Singh − *Faculty of Food and Land Systems, The University of British Columbia, Vancouver V6T 1Z4, Canada;* orcid.org/0000-0003-1752-0101

Complete contact information is available at: https://pubs.acs.org/10.1021/acsomega.4c03787

Notes

The authors declare no competing financial interest.

ACKNOWLEDGMENTS

The authors would like to thank Prof. John M. Frostad for allowing the use of the contact angle measurement device and Prof. Feng Jiang for the advice given on preliminary experiments. In addition, the authors would like to acknowledge the National Science and Engineering Research Council of Canada (NSERC) Alliance Grant (ALLRP 554607-20) and NSERC Discovery Research Grant (RGPIN-2018-04735) to Anubhav Pratap-Singh.

REFERENCES

(1) Mai-Prochnow, A.; Clauson, M.; Hong, J.; Murphy, A. B. Gram positive and Gram negative bacteria differ in their sensitivity to cold plasma. *Sci. Rep.* **2016**, *6* (1), 38610.

(2) Thirumdas, R.; Sarangapani, C.; Annapure, U. S. Cold plasma: a novel non-thermal technology for food processing. *Food Biophysics* **2015**, *10*, 1−11.

(3) Pankaj, S. K.; Bueno-Ferrer, C.; Misra, N.; Milosavljević, V.; O'donnell, C.; Bourke, P.; Keener, K.; Cullen, P. Applications of cold plasma technology in food packaging. *Trends in Food Science & Technology* **2014**, *35* (1), 5−17.

(4) Nicol, M. J.; Brubaker, T. R.; Honish, B. J.; Simmons, A. N.; Kazemi, A.; Geissel, M. A.; Whalen, C. T.; Siedlecki, C. A.; Bilén, S. G.; Knecht, S. D.; Kirimanjeswara, G. S. Antibacterial effects of low-temperature plasma generated by atmospheric-pressure plasma jet are mediated by reactive oxygen species. *Sci. Rep.* **2020**, *10* (1), 3066.

(5) Kar, R.; Chand, N.; Bute, A.; Maiti, N.; Rao, A. N.; Nagar, V.; Shashidhar, R.; Patil, D.; Ghosh, S.; Sharma, A. Cold plasma: Clean technology to destroy pathogenic micro-organisms. *Transactions of the Indian National Academy of Engineering* **2020**, *5*, 327−331.

(6) Filipić, A.; Gutierrez-Aguirre, I.; Primc, G.; Mozetič, M.; Dobnik, D. Cold plasma, a new hope in the field of virus inactivation. *Trends Biotechnol.* **2020**, *38* (11), 1278−1291.

(7) Gholamazad, A.; Hosseini, S.; Hosseini, S.; Ramezan, Y.; Rahmanabadi, A. Effect of low-pressure cold plasma on the properties of edible film based on alginate enriched with Dunaliella salina powder. *Plasma Process. Polym.* **2022**, *19* (5), No. 2100118.

(8) Macedo, M. J.; Silva, G. S.; Feitor, M. C.; Costa, T. H.; Ito, E. N.; Melo, J. D. Surface modification of kapok fibers by cold plasma surface treatment. *Journal of Materials Research and Technology* **2020**, *9* (2), 2467−2476.

(9) Yoshinari, M.; Wei, J.; Matsuzaka, K.; Inoue, T. Effect of cold plasma-surface modification on surface wettability and initial cell attachment. *Int. J Biomed. Biol. Eng.* **2009**, *3* (10), 507−511.

(10) Chizoba Ekezie, F. G.; Sun, D. W.; Cheng, J. H. A review on recent advances in cold plasma technology for the food industry: Current applications and future trends. *Trends Food Sci. Technol.* **2017**, *69*, 46−58.

(11) Hu, S.; Li, P.; Wei, Z.; Wang, J.; Wang, H.; Wang, Z. Antimicrobial activity of nisin-coated polylactic acid film facilitated by cold plasma treatment. *J. Appl. Polym. Sci.* **2018**, *135* (47), 46844.

(12) Hoque, M.; McDonagh, C.; Tiwari, B. K.; Kerry, J. P.; Pathania, S. Effect of cold plasma treatment on the packaging properties of biopolymer-based films: a review. *Applied Sciences* **2022**, *12* (3), 1346.

(13) Ucar, Y.; Ceylan, Z.; Durmus, M.; Tomar, O.; Cetinkaya, T. Application of cold plasma technology in the food industry and its combination with other emerging technologies. *Trends in Food Science & Technology* **2021**, *114*, 355−371.
(14) Cheng, X.; Murphy, W.; Recek, N.; Yan, D.; Cvelbar, U.; Vesel, A.; Mozetič, M.; Canady, J.; Keidar, M.; Sherman, J. H. Synergistic effect of gold nanoparticles and cold plasma on glioblastoma cancer therapy. *J. Phys. D: Appl. Phys.* **2014**, *47* (33), No. 335402.
(15) Chang, R.; Ji, N.; Li, M.; Qiu, L.; Sun, C.; Bian, X.; Qiu, H.; Xiong, L.; Sun, Q. Green preparation and characterization of starch nanoparticles using a vacuum cold plasma process combined with ultrasonication treatment. *Ultrasonics Sonochemistry* **2019**, *58*, No. 104660.
(16) Chang, R.; Lu, H.; Tian, Y.; Li, H.; Wang, J.; Jin, Z. Structural modification and functional improvement of starch nanoparticles using vacuum cold plasma. *Int. J. Biol. Macromol.* **2020**, *145*, 197−206.
(17) Babajani, A.; Iranbakhsh, A.; Oraghi Ardebili, Z.; Eslami, B. Seed priming with non-thermal plasma modified plant reactions to selenium or zinc oxide nanoparticles: cold plasma as a novel emerging tool for plant science. *Plasma Chemistry and Plasma Processing* **2019**, *39*, 21−34.
(18) Khatabi, H.; Bidoki, S. M.; Haji, A. A green approach for In-situ synthesis of silver nanoparticles on cotton fabric by low pressure cold plasma. *Mater. Chem. Phys.* **2022**, *290*, No. 126548.
(19) Wang, J.; Yu, Y.-D.; Zhang, Z.-G.; Wu, W.-C.; Sun, P.-L.; Cai, M.; Yang, K. Formation of sweet potato starch nanoparticles by ultrasonic—assisted nanoprecipitation: Effect of cold plasma treatment. *Frontiers in Bioengineering and Biotechnology* **2022**, *10*, No. 986033.
(20) Yoshinari, M.; Matsuzaka, K.; Inoue, T. Surface modification by cold-plasma technique for dental implants—Bio-functionalization with binding pharmaceuticals. *Japanese Dental Science Review* **2011**, *47* (2), 89−101.
(21) Ejtemaei, M.; Sadighi, S.; Rashidzadeh, M.; Khorram, S.; Back, J. O.; Penner, S.; Noisternig, M. F.; Salari, D.; Niaei, A. Investigating the cold plasma surface modification of kaolin-and attapulgite-bound zeolite A. *Journal of Industrial and Engineering Chemistry* **2022**, *106*, 113−127.
(22) Shapira, Y.; Chaniel, G.; Bormashenko, E. Surface charging by the cold plasma discharge of lentil and pepper seeds in comparison with polymers. *Colloids Surf., B* **2018**, *172*, 541−544.
(23) Chen, G.; Dong, S.; Zhao, S.; Li, S.; Chen, Y. Improving functional properties of zein film via compositing with chitosan and cold plasma treatment. *Industrial Crops and Products* **2019**, *129*, 318−326.
(24) Dong, S.; Guo, P.; Chen, Y.; Chen, G.-y.; Ji, H.; Ran, Y.; Li, S.-h.; Chen, Y. Surface modification via atmospheric cold plasma (ACP): Improved functional properties and characterization of zein film. *Industrial Crops and Products* **2018**, *115*, 124−133.
(25) Piskin, E.; Tuncel, A.; Denizli, A.; Ayhan, H. Monosize microbeads based on polystyrene and their modified forms for some selected medical and biological applications. *Journal of Biomaterials Science, Polymer Edition* **1994**, *5* (5), 451−471.
(26) Saralidze, K.; Koole, L. H.; Knetsch, M. L. Polymeric microspheres for medical applications. *Materials* **2010**, *3* (6), 3537−3564.
(27) Letícia Braz, A.; Ahmed, I. Manufacturing processes for polymeric micro and nanoparticles and their biomedical applications. *AIMS Bioeng.* **2017**, *4* (1), 46−72.
(28) Baldelli, A.; Vehring, R. Analysis of cohesion forces between monodisperse microparticles with rough surfaces. *Colloids Surf., A* **2016**, *506*, 179−189.
(29) Raj, H.; Sharma, A.; Sharma, S.; Verma, K. K.; Chaudhary, A. Mucoadhesive Microspheres: A Targeted Drug Delivery System. *Journal of Drug Delivery and Therapeutics* **2021**, *11* (2-S), 150−155.
(30) Baldelli, A.; Cidem, A.; Guo, Y.; Ong, H. X.; Singh, A.; Traini, D.; Pratap-Singh, A. Spray freeze drying for protein encapsulation: Impact of the formulation to morphology and stability. *Drying Technology* **2023**, *41* (1), 137−50.
(31) Pawar, O.; Deshpande, N.; Dagade, S.; Waghmode, S.; Nigam Joshi, P. Green synthesis of silver nanoparticles from purple acid phosphatase apoenzyme isolated from a new source Limonia acidissima. *Journal of Experimental Nanoscience* **2016**, *11* (1), 28−37.
(32) Segeren, L.; Siebum, B.; Karssenberg, F.; Van den Berg, J.; Vancso, G. J. microparticle adhesion studies by atomic force microscopy. *J. Adhes. Sci. Technol.* **2002**, *16* (7), 793−828.
(33) Mishra, M.; Mishra, B. Mucoadhesive microparticles as potential carriers in inhalation delivery of doxycycline hyclate: a comparative study. *Acta Pharmaceutica Sinica B* **2012**, *2* (5), 518−526.
(34) Di, A.; Zhang, S.; Liu, X.; Tong, Z.; Sun, S.; Tang, Z.; Chen, X. D.; Wu, W. D. Microfluidic spray dried and spray freeze dried uniform microparticles potentially for intranasal drug delivery and controlled release. *Powder Technol.* **2021**, *379*, 144−153.
(35) Liu, X.; Yan, S.; Li, M.; Zhang, S.; Guo, G.; Yin, Q.; Tong, Z.; Chen, X. D.; Wu, W. D. Spray dried levodopa-doped powder potentially for intranasal delivery. *Pharmaceutics* **2022**, *14* (7), 1384.
(36) Baldelli, A.; Boraey, M. A.; Oguzlu, H.; Cidem, A.; Rodriguez, A. P.; Ong, H. X.; Jiang, F.; Bacca, M.; Thamboo, A.; Traini, D.; Pratap-Singh, A. Engineered nasal dry powder for the encapsulation of bioactive compounds. *Drug Discovery Today* **2022**, *27* (8), 2300−2308.
(37) Baldelli, A.; Vehring, R. Control of the radial distribution of chemical components in spray-dried crystalline microparticles. *Aerosol Sci. Technol.* **2016**, *50* (10), 1130−1142.
(38) Zamankhan, P.; Ahmadi, G.; Wang, Z.; Hopke, P. K.; Cheng, Y.-S.; Su, W. C.; Leonard, D. Airflow and deposition of nano-particles in a human nasal cavity. *Aerosol Sci. Technol.* **2006**, *40* (6), 463−476.
(39) Fuller, K. N. G.; Tabor, D. The effect of surface roughness on the adhesion of elastic solids. *Proc. R. Soc. Lond. A* **1975**, *345* (1642), 327−342.
(40) Persson, B.; Tosatti, E. The effect of surface roughness on the adhesion of elastic solids. *J. Chem. Phys.* **2001**, *115* (12), 5597−5610.
(41) Xiao, J.; Lu, Q.; Cong, H.; Shen, Y.; Yu, B. Microporous poly (glycidyl methacrylate-co-ethylene glycol dimethyl acrylate) microspheres: synthesis, functionalization and applications. *Polym. Chem.* **2021**, *12* (42), 6050−6070.
(42) Song, S.-H.; Lee, J. H.; Yoon, J.; Park, W. Functional microparticle R&D for IVD and cell therapeutic technology: large-scale commercialized products. *BioChip Journal* **2019**, *13*, 95−104.
(43) Baldelli, A.; Trivanovic, U.; Sipkens, T. A.; Rogak, S. N. On determining soot maturity: A review of the role of microscopy-and spectroscopy-based techniques. *Chemosphere* **2020**, No. 126532.
(44) Baldelli, A.; Oguzlu, H.; Liang, D. Y.; Subiantoro, A.; Woo, M. W.; Pratap-Singh, A. Spray freeze drying of dairy products: Effect of formulation on dispersibility. *Journal of Food Engineering* **2022**, *335*, No. 111191.
(45) Jiang, J.; Zhu, Y.; Zargar, S.; Wu, J.; Oguzlu, H.; Baldelli, A.; Yu, Z.; Saddler, J.; Sun, R.; Tu, Q.; Jiang, F. Rapid, high-yield production of lignin-containing cellulose nanocrystals using recyclable oxalic acid dihydrate. *Ind. Crops Prod.* **2021**, *173*, No. 114148.
(46) Schug, C.; Schempp, S.; Lamparter, P.; Steeb, S. Surface roughness of sputter-deposited gold films: a combined x-ray technique and AFM study. *Surf. Interface Anal.* **1999**, *27* (7), 670−677.
(47) Guo, Y.; Baldelli, A.; Singh, A.; Fathordoobady, F.; Kitts, D.; Pratap-Singh, A. Production of high loading insulin nanoparticles suitable for oral delivery by spray drying and freeze drying techniques. *Sci. Rep.* **2022**, *12* (1), 9949.
(48) Fang, J.; Xuan, Y.; Li, Q. Preparation of polystyrene spheres in different particle sizes and assembly of the PS colloidal crystals. *Science China Technological Sciences* **2010**, *53*, 3088−3093.
(49) Wang, R.; Guo, W.; Li, X.; Liu, Z.; Liu, H.; Ding, S. Highly efficient MOF-based self-propelled micromotors for water purification. *RSC Adv.* **2017**, *7* (67), 42462−42467.
(50) Baldelli, A.; Ou, J.; Barona, D.; Li, W.; Amirfazli, A. Sprayable, superhydrophobic, electrically, and thermally conductive coating. *Adv. Mater. Interfaces* **2021**, *8* (2), No. 1902110.

https://doi.org/10.1021/acsomega.4c03787
ACS Omega 2024, 9, 35634−35644

(51) Baldelli, A.; Liang, D. Y.; Guo, Y.; Pratap-Singh, A. Effect of the formulation on mucoadhesive spray-dried microparticles containing iron for food fortification. *Food Hydrocolloids* **2022**, No. 107906.
(52) Brako, F.; Thorogate, R.; Mahalingam, S.; Raimi-Abraham, B.; Craig, D. Q.; Edirisinghe, M. Mucoadhesion of progesterone-loaded drug delivery nanofiber constructs. *ACS Appl. Mater. Interfaces* **2018**, *10* (16), 13381−13389.
(53) Rahul, B. S.; Lakshmi, S.; Sneha Letha, S.; Sidharth Mohan, M.; Rosemary, M. J. Mucoadhesive microspheres of ferrous sulphate−A novel approach for oral iron delivery in treating anemia. *Colloids Surf., B* **2020**, *195*, No. 111247.
(54) Woertz, C.; Preis, M.; Breitkreutz, J.; Kleinebudde, P. Assessment of test methods evaluating mucoadhesive polymers and dosage forms: An overview. *Eur. J. Pharm. Biopharm.* **2013**, *85* (3), 843−853.
(55) Saunders, M.; Jones, N.; Kabala, J.; Lowe, J. An anatomical, histological and magnetic resonance imaging study of the nasal septum. *Clinical Otolaryngology & Allied Sciences* **1995**, *20* (5), 434−438.
(56) Sanchis, M.; Calvo, O.; Fenollar, O.; Garcia, D.; Balart, R. Characterization of the surface changes and the aging effects of low-pressure nitrogen plasma treatment in a polyurethane film. *Polym. Test.* **2008**, *27* (1), 75−83.
(57) Fatyeyeva, K.; Dahi, A.; Chappey, C.; Langevin, D.; Valleton, J.-M.; Poncin-Epaillard, F.; Marais, S. Effect of cold plasma treatment on surface properties and gas permeability of polyimide films. *RSC Adv.* **2014**, *4* (59), 31036−31046.
(58) Benes, E.; Groschl, M.; Nowotny, H.; Trampler, F.; Keijzer, T.; Bohm, H.; Radel, S.; Gherardini, L.; Hawkes, J.; Konig, R. In Ultrasonic separation of suspended particles, *2001 IEEE Ultrasonics Symposium. Proceedings. An International Symposium (Cat. No. 01CH37263)*; IEEE: 2001; pp 649−659.
(59) Oguzlu, H.; Danumah, C.; Boluk, Y. Colloidal behavior of aqueous cellulose nanocrystal suspensions. *Curr. Opin. Colloid Interface Sci.* **2017**, *29*, 46−56.
(60) Rymuszka, D.; Terpiłowski, K.; Borowski, P.; Holysz, L. Time-dependent changes of surface properties of polyether ether ketone caused by air plasma treatment. *Polym. Int.* **2016**, *65* (7), 827−834.
(61) Clogston, J. D.; Patri, A. K. Zeta potential measurement. *Characterization of Nanoparticles Intended for Drug Delivery* **2011**, *697*, 63−70.
(62) Akishev, Y.; Grushin, M.; Dyatko, N.; Kochetov, I.; Napartovich, A.; Trushkin, N.; Minh Duc, T.; Descours, S. Studies on cold plasma−polymer surface interaction by example of PP-and PET-films. *J. Phys. D: Appl. Phys.* **2008**, *41* (23), No. 235203.
(63) Dimitrakellis, P.; Gogolides, E. Hydrophobic and super-hydrophobic surfaces fabricated using atmospheric pressure cold plasma technology: A review. *Adv. Colloid Interface Sci.* **2018**, *254*, 1−21.
(64) Bormashenko, E.; Whyman, G.; Multanen, V.; Shulzinger, E.; Chaniel, G. Physical mechanisms of interaction of cold plasma with polymer surfaces. *J. Colloid Interface Sci.* **2015**, *448*, 175−179.
(65) Kausar, A. Fabrication and characteristics of poly (benzimidazole/fluoro/ether/siloxane/amide)/sulfonated polystyrene/silica nanoparticle-based proton exchange membranes doped with phosphoric acid. *International Journal of Polymeric Materials and Polymeric Biomaterials* **2015**, *64* (4), 184−191.
(66) Krundaeva, A.; De Bruyne, G.; Gagliardi, F.; Van Paepegem, W. FTIR analysis of bacterial mediated chemical changes in polystyrene foam. *Ann. Biol. Res.* **2016**, *7* (5), 61.
(67) Umamaheswari, S.; Murali, M. FTIR spectroscopic study of fungal degradation of poly (ethylene terephthalate) and polystyrene foam. *Chem. Eng.* **2013**, *64* (19), 159.
(68) Ryan, B. J.; Poduska, K. M. Roughness effects on contact angle measurements. *American Journal of Physics* **2008**, *76* (11), 1074−1077.
(69) Wenzel, R. N. Surface roughness and contact angle. *J. Phys. Chem.* **1949**, *53* (9), 1466−1467.
(70) Liu, H.; Wang, F.; Yang, D.; Ou, J.; Baldelli, A. Solar reflective superhydrophobic coatings with phase change function. *J. Alloys Compd.* **2023**, *953*, No. 170021.
(71) Peppas, N. A.; Buri, P. A. Surface, interfacial and molecular aspects of polymer bioadhesion on soft tissues. *J. Controlled Release* **1985**, *2*, 257−275.
(72) Ding, D.; Kundukad, B.; Somasundar, A.; Vijayan, S.; Khan, S. A.; Doyle, P. S. Design of mucoadhesive PLGA microparticles for ocular drug delivery. *ACS Applied Bio Materials* **2018**, *1* (3), 561−571.

https://doi.org/10.1021/acsomega.4c03787
ACS Omega 2024, 9, 35634−35644